

This article was downloaded by:

On: 23 January 2011

Access details: *Access Details: Free Access*

Publisher *Taylor & Francis*

Informa Ltd Registered in England and Wales Registered Number: 1072954 Registered office: Mortimer House, 37-41 Mortimer Street, London W1T 3JH, UK



Journal of Coordination Chemistry

Publication details, including instructions for authors and subscription information:

<http://www.informaworld.com/smpp/title~content=t713455674>

Synthesis, characterization and crystal structures of Nickel(II) complexes containing sterically hindering Benzimidazole ligands

Philip D. Bauer^a; Mark S. Mashuta^a; Robert J. O'Brien^a; John F. Richardson^a; Robert M. Buchanan^a

^a Department of Chemistry, University of Louisville, Louisville, KY 40292, USA

To cite this Article Bauer, Philip D. , Mashuta, Mark S. , O'Brien, Robert J. , Richardson, John F. and Buchanan, Robert M.(2004) 'Synthesis, characterization and crystal structures of Nickel(II) complexes containing sterically hindering Benzimidazole ligands', *Journal of Coordination Chemistry*, 57: 5, 361 – 372

To link to this Article: DOI: 10.1080/00958970410001680345

URL: <http://dx.doi.org/10.1080/00958970410001680345>

PLEASE SCROLL DOWN FOR ARTICLE

Full terms and conditions of use: <http://www.informaworld.com/terms-and-conditions-of-access.pdf>

This article may be used for research, teaching and private study purposes. Any substantial or systematic reproduction, re-distribution, re-selling, loan or sub-licensing, systematic supply or distribution in any form to anyone is expressly forbidden.

The publisher does not give any warranty express or implied or make any representation that the contents will be complete or accurate or up to date. The accuracy of any instructions, formulae and drug doses should be independently verified with primary sources. The publisher shall not be liable for any loss, actions, claims, proceedings, demand or costs or damages whatsoever or howsoever caused arising directly or indirectly in connection with or arising out of the use of this material.

SYNTHESIS, CHARACTERIZATION AND CRYSTAL STRUCTURES OF NICKEL(II) COMPLEXES CONTAINING STERICALLY HINDERING BENZIMIDAZOLE LIGANDS

PHILIP D. BAUER, MARK S. MASHUTA, ROBERT J. O'BRIEN,
JOHN F. RICHARDSON and ROBERT M. BUCHANAN*

*Department of Chemistry, University of Louisville,
2320 S. Brook St., Louisville, KY 40292, USA*

(Received 6 August 2003; Revised 9 October 2003; In final form 9 February 2004)

The synthesis, characterization, and crystal structures of two Ni(II) complexes with *N,N*-bis[2-(2'-benzimidazolyl)ethyl]amine (bbiea) (**1**) and *N,N*-bis[2-(1'-methyl-2'-benzimidazolyl)ethyl]amine (bmbea) (**2**) are reported. The nickel complex Ni(bbiea)(O₂C₂H₃)(ClO₄) (**3**) crystallizes in the space group *C2/c*, with *a* = 35.830(7), *b* = 14.130(3), *c* = 10.756(2) Å, and β = 103.04(3)°. Compound **4**, Ni(bmbea)(NO₃)₂, crystallizes in the space group *P2₁/c*, with *a* = 17.024(5), *b* = 16.516(4), *c* = 8.692(2) Å, and β = 91.31(2)°. In **3**, the bbiea ligand is coordinated to the Ni(II) ion in a facial conformation, whereas the bmbea ligand in **4** adopts meridonal geometry. Both complexes contain a single benzimidazole chelate and the remaining coordination sites are occupied by solvent molecules and/or counterions. Reactions involving large excesses of ligand-to-metal and different solvents produced only the mono-chelated complexes **3** and **4**. No evidence for formation of bis-chelated complexes with Ni(II) was observed by MALDI-TOF and ESI-mass spectroscopy. Ligand field parameters for **3** and **4** were determined to be 9606 and 9862 cm⁻¹, respectively.

Keywords: Benzimidazole; Nickel complexes; Steric hindrance; Crystal structure; Polyimidazole; Mass spectrometry

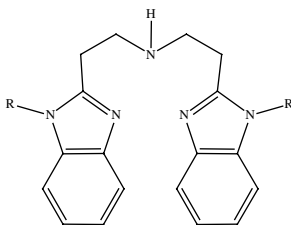
INTRODUCTION

Sterically hindered ligands have been used in a number of studies evaluating the effect of interligand steric interactions on the coordination environment of metal complexes [1–4]. Generally, ligands used in these studies have contained either bidentate, tridentate, or tetradentate frameworks, and have resulted in stabilization of mononuclear and polynuclear complexes. Hindered tridentate ligands are particularly useful in stabilizing complexes of lower nuclearity [5–9] and, in some instances, mononuclear complexes have been isolated containing solvent molecules or counterions included in the coordination environment.

*Corresponding author. Fax: 502-852-8149. E-mail: bob.buchanan@louisville.edu

Some of the best examples of this phenomenon include 1,4,7-triazacyclononane (tacn) and its derivative 1,4,7-trimethyl-1,4,7-triazacyclononane (Me₃tacn) [10]. The less hindered tacn ligand is capable of forming both bis-chelated and mono-chelated complexes of various metals [8,10–13]. The latter species exist as either mononuclear or bridged dinuclear compounds [14–16]. The more bulky 1,4,7-triisopropyl-1,4,7-triazacyclononane (*i*-Pr₃tacn) ligand also resists bis-chelation in favor of forming mono-chelated mononuclear complexes [17–19]. These results suggest that steric hindrance associated with N₃-tridentate ligands can be used to modulate the coordination environments of metal complexes favoring stabilization of mono-chelated over bis-chelated complexes.

With this in mind, we have focused on evaluating the crystal structures and properties of two structurally related N₃-tridentate benzimidazole ligands (**1**) that appear to stabilize only mono-chelated Ni(II) complexes. Compound **1**, *N,N*-bis[2-(2'-benzimidazolyl)ethyl]amine (bbiea), and compound **2**, *N,N*-bis[2-(1'-methyl-2'-benzimidazolyl)ethyl]amine (bmbea), have been reported to form complexes with copper [6,20]. Also, derivatives of these compounds have been used in copper binding studies [21–25]. However, their coordination chemistry with other metals is less well developed. Herein, we report the structures and properties of two related Ni(II) complexes of **1** and **2**, and examine the effect of benzimidazole ligand stereochemistry on the coordination environment of the metal.



bbiea R = H (**1**)
 bmbea R = CH₃ (**2**)

EXPERIMENTAL

Nickel(II) acetate tetrahydrate and nickel(II) nitrate hexahydrate were purchased from Merck and Fisher, respectively. Sodium perchlorate and reagent grade solvents were purchased from Aldrich and used as received. Elemental analyses were performed on dried samples by Midwest Microlabs, LLC. The ligands bbiea and bmbea were synthesized following previously published procedures [20].

Synthesis of [Ni(bbiea)(O₂C₂H₃)(CH₃OH)](ClO₄) (**3**)

Nickel(II) acetate tetrahydrate (0.171 g, 0.687 mmol) was added to a 20 cm³ methanol solution containing **1** (0.2034 g, 0.6660 mmol) and the reaction mixture was stirred

for 1 h. Sodium perchlorate (0.096 g, 0.79 mmol) was added to the blue reaction mixture and the solution was filtered. The filtrate was evaporated slowly under a stream of dry nitrogen yielding large blue crystals of **3** (0.187 g, 50% yield). Anal. Calcd. for $C_{21}H_{26}N_5O_7ClNi$ (%): C, 45.5; H, 4.7; N, 12.6. Found: C, 45.6; H, 4.7; N, 12.5. ESI-MS: $m/z = 422 [Ni(bbica)(O_2C_2H_3)]^+$. UV-Vis-near IR: $\lambda_{max} = 381, 628, \text{ and } 1041 \text{ nm}$.

Synthesis of $[Ni(\text{bmbea})(NO_3)_2]$ (**4**)

Nickel(II) nitrate hexahydrate (0.0968 g, 0.333 mmol) was dissolved in 4 cm^3 methanol and added dropwise with stirring to a 1 cm^3 methanol solution containing **2** (0.1131 g, 0.339 mmol). The resulting blue reaction mixture was stirred for 15 min and allowed to stand for 24 h, after which a light-blue powder was isolated by filtration (0.1224 g, 71% yield). X-ray quality crystals of **4** were obtained by vapor diffusion of Et_2O into a 1:1 methanol/acetonitrile solution containing 7.2 mg of the blue powder. Anal. Calcd. for $C_{20}H_{23}N_7O_6Ni$ (%): C, 46.5; H, 4.5; N, 19.0. Found: C, 46.5; H, 4.7; N, 19.2. ESI-MS: $m/z = 453 [Ni(\text{bmbea})(NO_3)]^+$. UV-Vis-near IR: $\lambda_{max} = 376, 615, \text{ and } 1014 \text{ nm}$.

Physical Measurements

UV-Vis-near-IR spectra were measured on an Agilent Spectrophotometer Model 8453, between 190 and 1100 nm. Spectra were recorded on compounds **3** and **4** dissolved in methanol and 1:1 methanol/acetonitrile solutions, respectively. Mass spectra were recorded using MALDI-TOF and ESI-MS methods. MALDI-TOF (Matrix Assisted Laser Desorption Ionization – Time Of Flight) spectra were obtained using a Perspective Biosystems Instrument Model 6032 Voyager-DE PRO mass spectrometer over the m/z range 120–1000, using 256 shots per spectrum. Samples were prepared by dissolving approximately 1 mg of sample in 1:1 methanol/dichloromethane and mixing with a solution of dithranol (dith) in the same solvent. ESI-MS (Electrospray Ionization Mass Spectrometry) spectra were recorded using a Micromass Quattro LCZ triple quadrupole electrospray ionization mass spectrometer. 0.1 mM samples were prepared and injected at a rate of $0.20 \text{ cm}^3/\text{h}$.

X-ray Crystallography

Data were collected on a Nonius CAD4 diffractometer at 298 K. Crystal data and pertinent details of the structure refinement of **3** and **4** are given in Table I. The structures were solved by Patterson methods [26] and refined on F^2 using SHELXTL (v. 6.12) [27,28]. Additional information on data collection and structure solution is provided for individual structures below.

For a single crystal of **3** mounted on a glass fiber and coated with epoxy, the final least-squares refinement for 378 variables using 4660 (all) data converged at $R_1 = 0.063$, $wR_2 = 0.117$, and $GOF = 1.039$. The oxygen atoms of the perchlorate anion are disordered and are accurately modeled with two sets of four half-occupancy O-atoms [O(4a)–O(7a) and O(4b)–O(7b)], each refined anisotropically using the SADI restraint. A disordered methanol solvate present in the lattice was modeled using one anisotropically refined full-occupancy oxygen atom [O(50)] and four 25%-occupancy carbon atoms [C(50a)–C(50d)] refined isotropically. All other non-hydrogen atoms

TABLE I Crystal data and structure refinement details for **3** and **4**

	3	4
Empirical formula	C ₂₁ H ₂₀ ClN ₅ NiO ₇ ·1.0[CH ₃ OH]	C ₂₀ H ₂₃ N ₇ NiO ₆ ·1.0[CH ₃ CN]
Formula weight	580.62	557.22
Temperature (K)	293(2)	293(2)
Wavelength (Å)	0.71073	0.71073
Crystal sample	Monoclinic	Monoclinic
Space group	C2/c	P2 ₁ /c
Unit cell dimensions (Å, °)	<i>a</i> = 35.830(7) <i>b</i> = 14.130(3) <i>c</i> = 10.756(2) β = 103.04(3)	<i>a</i> = 17.024(5) <i>b</i> = 16.516(4) <i>c</i> = 8.692(2) β = 91.31(2)
<i>V</i> (Å ³)	5305(2)	2443.3(8)
<i>Z</i>	8	4
Density (calc) (Mg m ⁻³)	1.454	1.515
Absorption coefficient (mm ⁻¹)	0.886	0.850
<i>F</i> (000)	2400	1160
Crystal size (mm ³)	0.45 × 0.30 × 0.30	0.30 × 0.28 × 0.23
Crystal color (habit)	Green block	Turquoise block
Diffractometer	CAD4	CAD4
Scan type	ω -2 θ	ω -2 θ
θ range for data collection (°)	2.27 to 24.97	2.39 to 25.03
Index ranges	-42 ≤ <i>h</i> ≤ 42 0 ≤ <i>k</i> ≤ 16 0 ≤ <i>l</i> ≤ 12	-20 ≤ <i>h</i> ≤ 20 -19 ≤ <i>k</i> ≤ 19 -10 ≤ <i>l</i> ≤ 10
Reflections collected	4943	8628
Independent reflections	4660 [<i>R</i> (int) = 0.0110]	4317 [<i>R</i> (int) = 0.0315]
Completeness to θ	99.9%	99.7%
Absorption correction	Empirical ψ -scans	Empirical ψ -scans
Max. and min. transmission	0.8029 and 0.7229	0.7919 and 0.7260
Refinement method	Full-matrix least-squares on <i>F</i> ²	Full-matrix least-squares on <i>F</i> ²
Data/restraints/parameters	4660/6/378	4317/0/353
Goodness-of-fit on <i>F</i> ²	1.039	1.004
Final <i>R</i> indices [<i>I</i> > 2 σ (<i>I</i>)]	<i>R</i> 1 ^a = 0.0462 <i>wR</i> 2 ^b = 0.1088	<i>R</i> 1 ^a = 0.0461 <i>wR</i> 2 ^b = 0.1037
<i>R</i> indices (all data)	<i>R</i> 1 = 0.0628 <i>wR</i> 2 = 0.1168	<i>R</i> 1 = 0.0782 <i>wR</i> 2 = 0.1166
Extinction coefficient	0.00421(17)	0.0049(3)
Largest diff. peak and hole (e Å ⁻³)	0.701 and -0.575	0.736 and -0.269

^a*R*1 = $\sum ||F_o| - |F_c|| / \sum |F_o|$; ^b*wR*2 = $\{\sum [w(F_o^2 - F_c^2)^2] / \sum w(F_o^2)^2\}^{1/2}$ where $q/\sigma^2(F_o^2) + (ap)^2 + bp$.

were refined anisotropically. Hydrogen atom positions were calculated and refined using riding models with $U(\text{H}) = 1.2 U_{\text{eq}}$ (attached atom) for methylene, amine, benzimidazole C–H and benzimidazole N–H hydrogen atoms. $U(\text{H}) = 1.5 U_{\text{eq}}$ for all CH₃ hydrogen atoms.

A single crystal of **4** was mounted in a capillary with the mother liquor from the crystallization solution for data collection. For **4**, a nitrate bound monodentately to the nickel atom was modeled for disorder, in which two of the oxygen atoms [O(4a)–O(5a) and O(4b)–O(5b)] of the nitrate were modeled at 60 and 40% occupancy, respectively. All non-hydrogen atoms were refined anisotropically. One hydrogen atom associated with the amine nitrogen was found by difference maps. All other hydrogen atoms were calculated for ideal positions and treated as riding models, as described above for **3**. For 353 variables using 4317 unique reflections (all data) and refinement of *F*², the discrepancy indices are *R*₁ = 0.078 and *wR*₂ = 0.117 with a GOF = 1.004.

RESULTS AND DISCUSSION

Synthesis of Metal Complexes

Compounds **3** and **4** were prepared using a 1 : 1 ligand-to-metal stoichiometry in methanol. The resulting mono-chelated complexes were isolated in reasonable yields and have limited solubility in methanol, rapidly precipitating upon formation as pale-blue solids. Interestingly, when the ligand-to-metal ratios were varied between 2 : 1 and 10 : 1, compounds **3** and **4** were the only species isolated. In order to evaluate the role of methanol in the reactions, the solvent medium was changed to a 1 : 1 methanol/acetonitrile mixture in which both **3** and **4** are soluble. This solvent combination should minimize the effect of ion pairing on the metal–chelate stoichiometry of the resulting Ni(II) products. Once again, only the mono-chelated complexes **3** and **4** were isolated, or detected by mass spectrometry (*vide infra*) in reaction mixtures containing the above range of ligand-to-metal stoichiometries. It appears that the above changes in the reaction conditions do not significantly influence the metal–ligand stoichiometries of the isolated Ni(II) complexes. Also, addition of excess **1** and **2** to 1 : 1 methanol/acetonitrile solutions containing **3** and **4**, respectively, failed to produce detectable quantities of bis-chelated Ni(II) complexes.

Mass Spectrometry

The structure and stability of compounds **3** and **4** in solution were studied using ESI and MALDI-TOF mass spectrometry. None of the Ni(II) complexes displayed the expected $[M]^+$ and $[M + H]^+$ ions generally observed for either technique [29–31]. The ESI mass spectrum of **3** (Fig. 1a) displays a peak at m/z 422 assigned to the $[\text{Ni}(\text{bbica})(\text{OAc})]^+$ ion which results from the loss of CH_3OH from the parent compound. This result suggests that the methanol ligand in **3** may be labile and susceptible to ligand displacement reactions. In addition, a minor peak was observed at m/z 362,

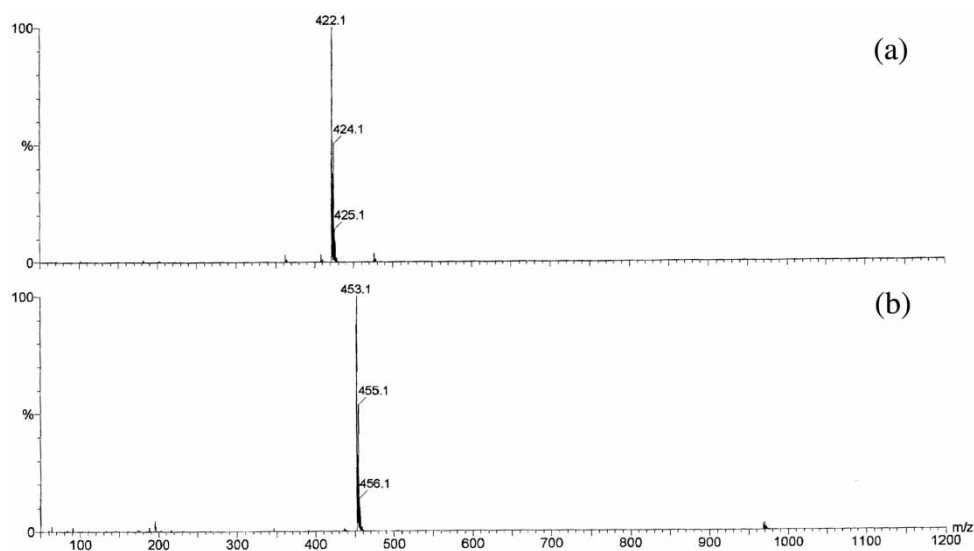


FIGURE 1 (a) ESI-MS spectrum of compound **3**; (b) ESI-MS spectrum for compound **4**.

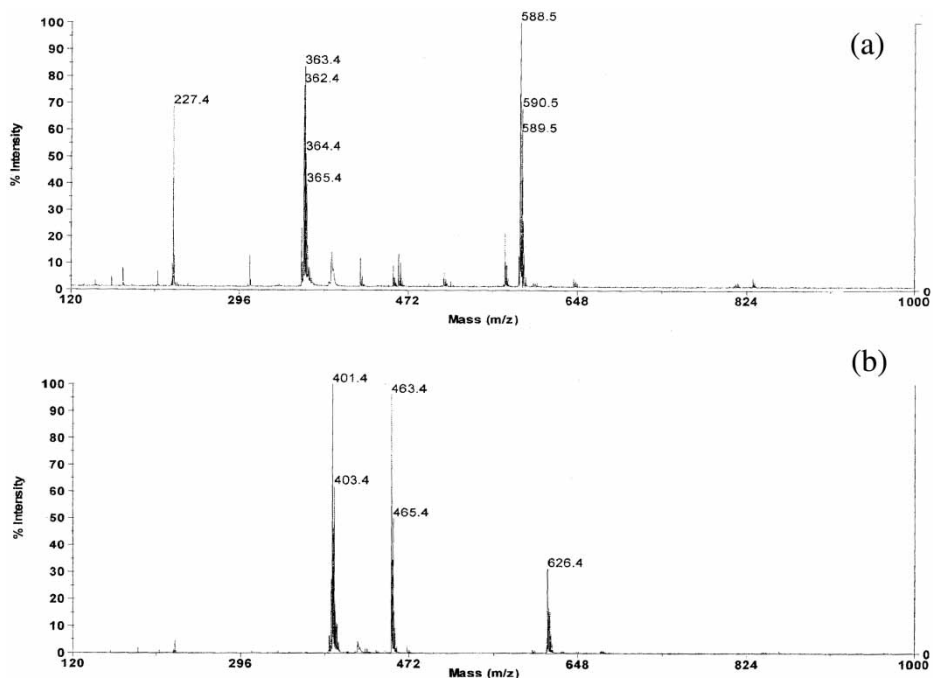


FIGURE 2 (a) MALDI-TOF spectrum of compound **3**; (b) MALDI-TOF spectrum for compound **4**.

assigned to the $[\text{Ni}(\text{bbica} - \text{H})]^+$ ion. The bbica ligand contains two types of ionizable N–H hydrogen atoms associated with the benzimidazole and amine groups.

The MALDI-TOF mass spectrum of **3** (Fig. 2a), on the other hand, is more complicated due to the presence of the dithranol matrix. The highest mass ion peak was observed at m/z 589 and is assigned to the $[\text{Ni}(\text{bbica})(\text{dith})]^+$ ion. Apparently, the dithranol anion coordinates with the Ni(II) displacing both the methanol and acetate ligands prior to ionization. As with ESI-MS, a peak was observed at m/z 422 for the $[\text{Ni}(\text{bbica})(\text{OAc})]^+$, as well as minor peaks at m/z 362 and 363 assigned to the $[\text{Ni}(\text{bbica} - \text{H})]^+$ and $[\text{Ni}(\text{bbica})]^+$ ions, respectively.

The ESI mass spectrum of **4** is shown in Fig. 1(b). Unlike for compound **3**, only one major peak is observed in the spectrum of **4** at m/z 453, assigned to the $[\text{Ni}(\text{bmbea})(\text{NO}_3)]^+$ ion. It is interesting that a peak at m/z 390, expected for the $[\text{Ni}(\text{bmbea} - \text{H})]^+$ ion, was not observed in the ESI spectrum of **4**. The bmbea ligand lacks benzimidazole N–H hydrogen atoms, but does contain amine H-atoms. Therefore, it appears that the $[\text{Ni}(\text{bbica} - \text{H})]^+$ ion associated with **3** is likely generated by the loss of a benzimidazole H^+ ion.

As with compound **3**, the MALDI-TOF mass spectrum of **4** (Fig. 2b) was more complicated than the ESI spectrum. Mass ions were observed at m/z 401 ($[\text{Ni}(\text{bmbea})]^+$), 463 ($[\text{Ni}(\text{bmbea})(\text{NO}_3)]^+$), and 626 ($[\text{Ni}(\text{bmbea})(\text{dith})]^+$). The most abundant mass ion was associated with the $[\text{Ni}(\text{bmbea})]^+$ species.

Both mass spectral methods were also employed in analyzing the products from reactions in 1:1 methanol/acetonitrile involving ligand-to-metal ratios ranging from 2:1 to 10:1, and from all of the solutions analyzed, only mass ions of the mono-chelated species above were detected. More importantly, mass ions at m/z 667

[Ni(bbica)(bbica-H)]⁺, 334 [Ni(bbica)₂]²⁺, and 723 [Ni(bmbea)(bmbea-H)]⁺, 362 [Ni(bmbea)₂]²⁺ were not observed in the control studies.

X-ray Crystallography

The X-ray crystal structures of compounds **3** and **4** confirm 1:1 ligand-to-metal stoichiometry of the Ni(II) complexes and differences in the conformations of the N₃ chelates. Pertinent bond distances and angles of **3** and **4** are listed in Tables II and III, respectively.

An ORTEP representation of **3** is shown in Fig. 3. The nickel atom is coordinated to a bbica chelate, an acetate ion, and a methanol ligand. The overall coordination environment of the nickel atom is best described as distorted octahedral. The bbica ligand is facially coordinated to the Ni(II) through two benzimidazole N atoms

TABLE II Selected bond lengths (Å) and angles (°) for **3**

<i>Bond lengths</i>		<i>Bond angles</i>	
Ni(1)–N(1)	2.104(3)	N(1)–Ni(1)–N(2)	90.16(12)
Ni(1)–N(2)	2.049(3)	N(1)–Ni(1)–N(4)	94.97(12)
Ni(1)–N(4)	2.036(3)	N(2)–Ni(1)–N(4)	97.02(12)
Ni(1)–O(1)	2.093(3)	N(1)–Ni(1)–O(1)	163.07(11)
Ni(1)–O(2)	2.217(2)	N(1)–Ni(1)–O(2)	102.35(11)
Ni(1)–O(3)	2.133(3)	N(1)–Ni(1)–O(3)	86.14(11)
		N(2)–Ni(1)–O(1)	90.81(11)
		N(2)–Ni(1)–O(2)	86.09(11)
		N(2)–Ni(1)–O(3)	172.68(11)
		N(4)–Ni(1)–O(1)	101.68(11)
		N(4)–Ni(1)–O(2)	162.41(10)
		N(4)–Ni(1)–O(3)	89.60(11)
		O(1)–Ni(1)–O(2)	60.87(10)
		O(1)–Ni(1)–O(3)	90.90(11)
		O(2)–Ni(1)–O(3)	88.52(10)

TABLE III Selected bond lengths (Å) and angles (°) for **4**

<i>Bond lengths</i>		<i>Bond angles</i>	
Ni(1)–N(1)	2.060(4)	N(1)–Ni(1)–N(2)	92.95(13)
Ni(1)–N(2)	2.053(3)	N(1)–Ni(1)–N(4)	91.43(14)
Ni(1)–N(4)	2.052(3)	N(2)–Ni(1)–N(4)	173.05(13)
Ni(1)–O(1)	2.207(3)	N(1)–Ni(1)–O(1)	146.09(15)
Ni(1)–O(2)	2.199(4)	N(1)–Ni(1)–O(2)	89.27(15)
Ni(1)–O(4A)	2.037(8)	N(1)–Ni(1)–O(4A)	113.7(3)
Ni(1)–O(4B)	2.326(12)	N(1)–Ni(1)–O(4B)	75.2(3)
		N(2)–Ni(1)–O(1)	89.74(11)
		N(2)–Ni(1)–O(2)	91.90(13)
		N(2)–Ni(1)–O(4A)	89.4(3)
		N(2)–Ni(1)–O(4B)	82.9(3)
		N(4)–Ni(1)–O(1)	89.63(12)
		N(4)–Ni(1)–O(2)	93.55(13)
		N(4)–Ni(1)–O(4A)	83.9(3)
		N(4)–Ni(1)–O(4B)	93.0(3)
		O(1)–Ni(1)–O(4A)	100.2(3)
		O(1)–Ni(1)–O(4B)	138.6(3)
		O(2)–Ni(1)–O(4A)	157.0(3)
		O(2)–Ni(1)–O(4B)	163.3(3)

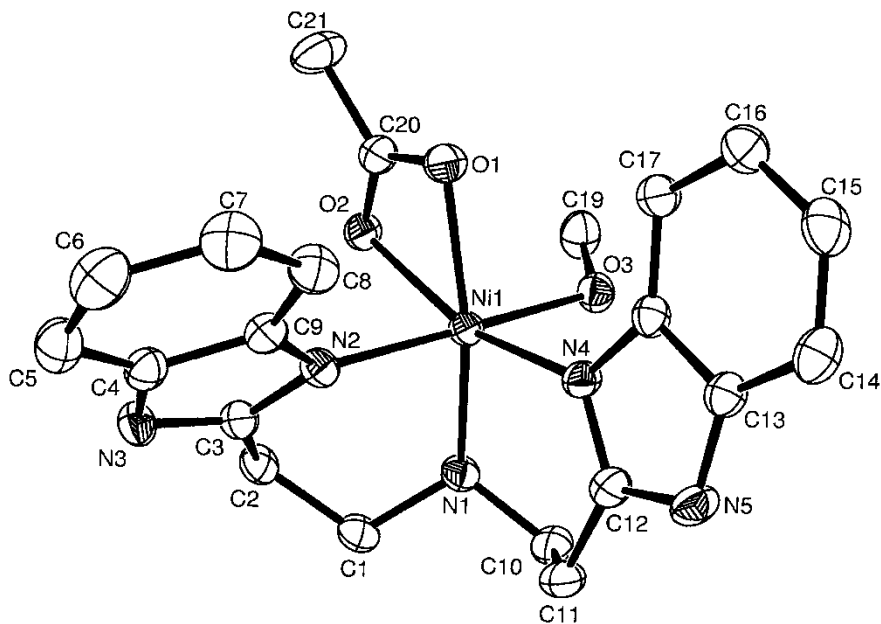


FIGURE 3 ORTEP-3 plot of the Ni subunit of **3** [32]. Thermal ellipsoids are shown at 50% probability. Hydrogen atoms bound to carbons are omitted for clarity. Hydrogen atom on N(1) is obscured by N(1).

TABLE IV Selected torsion angles for **3** and **4** (°)

	3	4
N(1)–Ni(1)–N(2)–C(3)	–38.82(26)	5.99(34)
N(1)–Ni(1)–N(4)–C(12)	–13.29(28)	–2.65(36)
Ni(1)–N(1)–C(1)–C(2)	27.87(39)	–67.93(47)
Ni(1)–N(1)–C(10)–C(11)	58.17(33)	62.50(57)
C(1)–C(2)–C(3)–N(2)	51.01(45)	–28.88(62)
C(10)–C(11)–C(12)–N(4)	39.94(48)	17.73(69)

[Ni–N(2) = 2.049(3) Å and Ni–N(4) = 2.036(3) Å] and an amine N atom [Ni–N(1) = 2.104(3) Å]. The remaining coordination sites are occupied by O atoms of the acetate ligand [Ni–O(1) = 2.093(3) Å and Ni–O(2) = 2.217(2) Å], and an O atom of the methanol ligand [Ni–O(3) = 2.133(3) Å]. The Ni–N and Ni–O distances are consistent with other N₃O₃ octahedral Ni(II) complexes containing benzimidazole ligands [5,33–35], and the N–Ni–N bond angles of the bbiea ligand deviate from 90°. Table IV displays selected torsion angles for **3**. The torsion angles for Ni(1)–N(1)–C(1)–C(2), Ni(1)–N(1)–C(10)–C(11), C(1)–C(2)–C(3)–N(2), and C(10)–C(11)–C(12)–N(4) indicate the strain associated with the backbone of the N₃-chelate in the facial conformation. In addition, the N(1)–Ni(1)–N(2)–C(3) and N(1)–Ni(1)–N(4)–C(12) angles show the twisting of the benzimidazole units relative to each other.

Figure 4 shows an ORTEP representation of compound **4**. As with **3**, compound **4** has distorted octahedral geometry. The nickel atom is coordinated to the bmbea chelate, a bidentate nitrate ligand and a monodentate nitrate ligand. The bmbea ligand is coordinated to the Ni atom through two benzimidazole nitrogen atoms [Ni–N(2) = 2.053(3) Å and Ni–N(4) = 2.052(3) Å] and an amine N atom [Ni–N(1) = 2.060(4) Å].

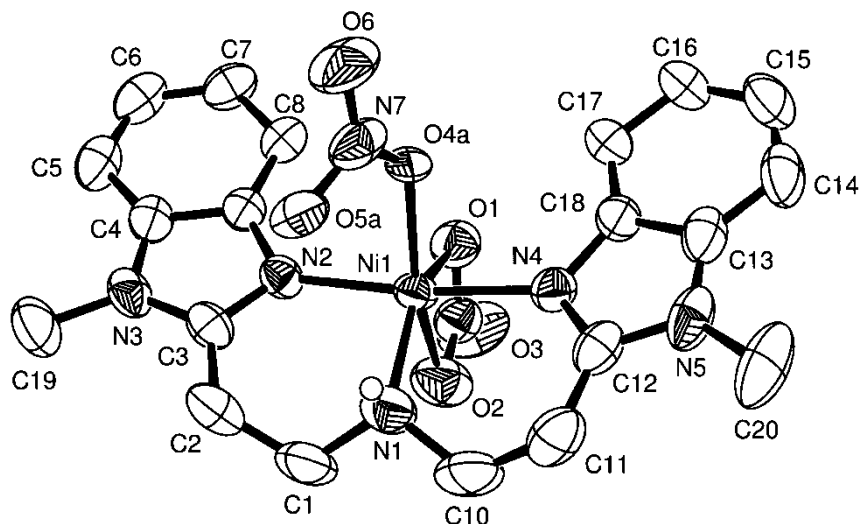


FIGURE 4 ORTEP-3 plot of the Ni subunit of **4** [32]. Thermal ellipsoids are shown at 50% probability. All hydrogen atoms bound to carbons have been omitted for clarity.

Unlike the *bbiea* ligand in **3**, the *bmbea* ligand in **4** adopts a meridional conformation. The N(4)–Ni–N(2) angle for **4** is 173.1(1)°, and the other N–Ni–N angles are close to 90°. The remaining coordination sites are occupied by two O atoms of the bidentate nitrate ligand [Ni–O(1) = 2.207(3) Å and Ni–O(2) = 2.199(4) Å] and an O atom of the monodentate nitrate ligand [Ni–O(4a) = 2.037(8) Å]. As with compound **3**, the Ni–N and Ni–O distances are consistent with other Ni(II) complexes containing benzimidazole ligands [5,33–35]. The hydrogen atoms associated with C(8) and C(17) are separated by a distance of 3.323 Å. This short distance may be important in retarding formation of bis-chelated complexes of **2** with Ni(II). Selected torsion angles for **4** are given in Table IV. The torsion angles, Ni(1)–N(1)–C(1)–C(2), Ni(1)–N(1)–C(10)–C(11), C(1)–C(2)–C(3)–N(2), and C(10)–C(11)–C(12)–N(4), show that both backbone units are bent to the same side of the meridional plane. Also, the torsion angles for N(1)–Ni(1)–N(2)–C(3) and N(1)–Ni(1)–N(4)–C(12) show that the benzimidazole units are twisted slightly out of the meridional plane, although they are less twisted than the *bbiea* ligand in **3**.

UV-Vis and Near-IR Spectroscopy

The UV-Vis spectra of compounds **3** and **4** (Fig. 5) are typical of Ni(II) complexes in a *pseudo*-octahedral environment [36]. Ni(II) complexes generally display three spin-allowed transitions, which fall in the ranges 7000–13 000, 11 000–20 000, and 19 000–27 000 cm⁻¹. The spectrum of **3** (Fig. 5a) in methanol displays peaks at 381 nm ($\epsilon = 29.4 \text{ M}^{-1} \text{ cm}^{-1}$), 628 nm ($\epsilon = 16.6 \text{ M}^{-1} \text{ cm}^{-1}$), and 1041 nm ($\epsilon = 8.1 \text{ M}^{-1} \text{ cm}^{-1}$), which correspond to the ${}^3\text{A}_{2g} \rightarrow {}^3\text{T}_{1g}(\text{P})$, ${}^3\text{A}_{2g} \rightarrow {}^3\text{T}_{1g}(\text{F})$, and ${}^3\text{A}_{2g} \rightarrow {}^3\text{T}_{2g}$ transitions, respectively. From the lowest energy transition (${}^3\text{A}_{2g} \rightarrow {}^3\text{T}_{2g}$), the ligand field parameter, Δ_0 , was determined to be 9606 cm⁻¹. The spectrum of **4** (Fig. 5b) in 1 : 1 methanol/acetonitrile also displays three peaks, at 376 nm ($\epsilon = 38.3 \text{ M}^{-1} \text{ cm}^{-1}$), 615 nm

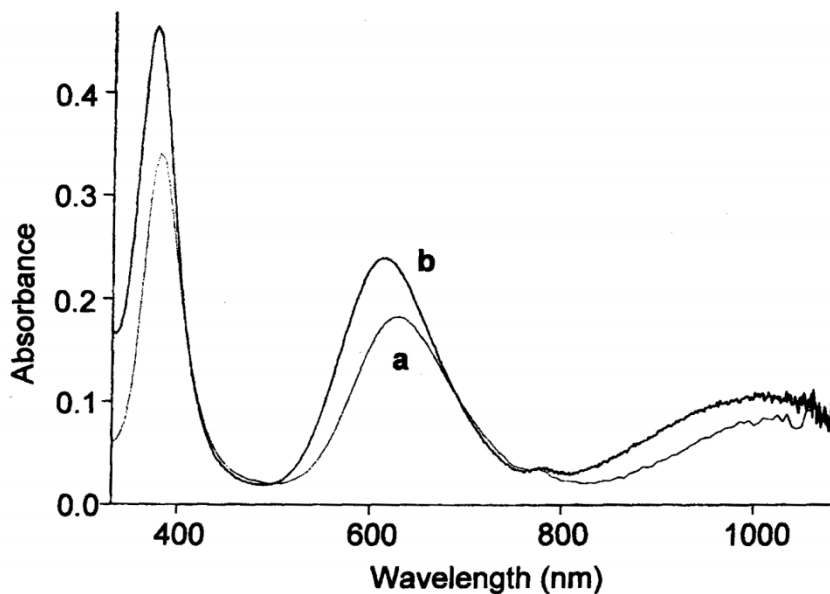


FIGURE 5 UV-Vis spectra for (a) **3** (10.8 mM in methanol) and (b) **4** (12.1 mM in 1 : 1 methanol/acetonitrile).

($\epsilon = 19.8 \text{ M}^{-1} \text{ cm}^{-1}$), and 1014 nm ($\epsilon = 9.09 \text{ M}^{-1} \text{ cm}^{-1}$), and Δ_0 was determined to be 9862 cm^{-1} [37].

CONCLUSIONS

The coordination properties of **1** and **2** with Ni(II) indicate that the N_3 -chelates are flexible enough to adopt both facial and meridional conformations. In addition, bis-chelation was not observed for either ligand, even though reactions were conducted using large quantities of excess ligand relative to Ni(II) salts, and in different reaction media. The latter observation is important and suggests the steric bulk of **1** and **2** hinder access of a second chelate during the course of the reaction. Interestingly, the related benzimidazole ligands, *N,N*-bis[(1-methyl-2-benzimidazolyl)methyl]amine (bmbma) and *N,N*-bis[(2-benzimidazolyl)methyl]amine (bbma) are known to form both mono- and bis-chelated complexes containing predominately facial chelate conformations with first row transition metals [33,38,39]. The only apparent difference between the two groups of ligands is the presence of ethylene amine linkers in **1** and **2** compared to methylene amine linkers in bbma and bmbma. Therefore, the greater conformational flexibility and size of **1** and **2** appear to regulate the number of chelates bonded to the Ni atoms in **3** and **4**. Future studies will explore the coordination chemistry of **1** and **2** with other metals and in the presence of non-coordinating anions to generate potentially labile coordination environments.

Acknowledgments

We would like to thank Dr. Craig Grapperhaus for the use of the UV-Vis-near IR spectrophotometer, and Dr. William Pierce and Ned Smith for their assistance with the ESI-MS.

Supplementary Material

Crystallographic data for both structures have been deposited with the Cambridge Crystallographic Data Centre as supplementary publication number CCDC 216067 (3) and CCDC 216068 (4). These data can be obtained free of charge via www.ccdc.cam.ac.uk/conts/retrieving.html (or from the Cambridge Crystallographic Data Centre, 12 Union Road, Cambridge, CB2 1EZ, UK; fax: (+44) 1223-336-033; or deposit@ccdc.cam.ac.uk). Other supplementary material, including isotopic models for mass spectral peaks, may be obtained upon request from the authors.

References

- [1] C.-M. Che, W.-Y. Yu, P.-M. Chan, W.-C. Cheng, S.-M. Peng, K.-C. Lau and W.-K. Li, *J. Am. Chem. Soc.* **122**, 11380 (2000).
- [2] G.B. Shul'pin, G.V. Nizova, Y.N. Kozlov and I.G. Pechenkina, *New J. Chem.* **26**, 1238 (2002).
- [3] J.-C. Hierso, R. Amardeil, E. Bentabet, R. Broussier, B. Gautheron, P. Meunier and P. Kalck, *Coord. Chem. Rev.* **236**, 143 (2003).
- [4] J.A.R. Navarro and B. Lippert, *Coord. Chem. Rev.* **222**, 219 (2001).
- [5] M. Soriano-García, T. Pandiyan and C. Durán de Bazúa, *Acta Crystallogr.* **C51**, 1107 (1995).
- [6] L. Casella, O. Carugo, M. Gullotti, S. Doldi and M. Frassoni, *Inorg. Chem.* **35**, 1101 (1996).
- [7] J.W.F.M. Schoonhoven, W.L. Driessen, J. Reedijk and G.C. Verschoor, *J. Chem. Soc., Dalton Trans.* 1053 (1984).
- [8] G.H. Searle, D.-N. Wang, S. Larsen and E. Larsen, *Acta Chem. Scand.* **46**, 38 (1992).
- [9] K. Takahashi and Y. Nishida, *Z. Naturforsch.* **42b**, 1307 (1987).
- [10] P. Chaudhuri and K. Wieghardt, *Progress in Inorganic Chemistry* (J. Wiley & Sons, New York, 1987), Vol. 35, p. 329.
- [11] R. Yang and L.J. Zompa, *Inorg. Chem.* **15**, 1499 (1976).
- [12] L.J. Zompa and T.N. Margulis, *Inorg. Chim. Acta* **28**, L157 (1978).
- [13] R. Stranger, S.C. Wallis, L.R. Gahan, C.H.L. Kennard and K.A. Byriel, *J. Chem. Soc., Dalton Trans.* 2971 (1992).
- [14] P. Chaudhuri, T. Weyhermüller, E. Bill and K. Wieghardt, *Inorg. Chim. Acta* **252**, 195 (1996).
- [15] P. Chaudhuri, H.-J. Küppers, K. Wieghardt, S. Gehring, W. Haase, B. Nuber and J. Weiss, *J. Chem. Soc. Dalton Trans.* 1367 (1988).
- [16] P. Chaudhuri, M. Guttman, D. Ventur, K. Wieghardt, B. Nuber and J. Weiss, *J. Chem. Soc. Chem. Commun.* 1618 (1985).
- [17] J.L. Sessler, J.W. Sibert and V. Lynch, *Inorg. Chim. Acta* **216**, 89 (1994).
- [18] A. Diebold, A. Elboudili and K.S. Hagen, *Inorg. Chem.* **39**, 3915 (2000).
- [19] B.M.T. Lam, J.A. Halfen, V.G. Young Jr., J.R. Hagadorn, P.L. Holland, A. Lledós, L. Cucurull-Sánchez, J.J. Novoa, S. Alvarez and W.B. Tolman, *Inorg. Chem.* **39**, 4059 (2000).
- [20] T.N. Sorrell and M.L. Garrity, *Inorg. Chem.* **30**, 210 (1991).
- [21] L. Santagostini, M. Gullotti, E. Monzani, L. Casella, R. Dillinger and F. Tuzcek, *Chem. Eur. J.* **6**, 519 (2000).
- [22] E. Monzani, L. Quinti, A. Perotti, L. Casella, M. Gullotti, L. Randaccio, S. Geremia, G. Nardin, P. Faleschini and G. Tabbi, *Inorg. Chem.* **37**, 553 (1998).
- [23] L. Casella, E. Monzani, M. Gullotti, D. Cavagnino, G. Cerina, L. Santagostini and R. Ugo, *Inorg. Chem.* **35**, 7516 (1996).
- [24] L. Casella, M. Gullotti, R. Radaelli and P. di Gennaro, *J. Chem. Soc., Chem. Commun.* 1611 (1991).
- [25] L. Casella, E. Monzani, M. Gullotti, F. Gliubich and L. de Gioia, *J. Chem. Soc., Dalton Trans.* 3203 (1994).
- [26] G.M. Sheldrick, *Acta Crystallogr.* **A46**, 467 (1990).
- [27] G.M. Sheldrick, *SHELXL-97*; Program for the Refinement of Crystal Structure (University of Göttingen, Göttingen, 1997).

- [28] SHELXTL, Version 6.12; Program Library for Structure Solution and Molecular Graphic (Bruker Advanced X-ray Solutions, Madison, WI, 2001).
- [29] M.A.R. Meier, B.G.G. Lohmeijer and U.S. Schubert, *J. Mass Spectrom.* **38**, 510 (2003).
- [30] G. Du, A. Ellern and L.K. Woo, *Inorg. Chem.* **42**, 873 (2003).
- [31] H.-F. Zhu, W.-Y. Sun, T.-A. Okamura and N. Ueyama, *Inorg. Chem. Comm.* **6**, 168 (2003).
- [32] L.J. Farrugia, *J. Appl. Crystallogr.* **30**, 565 (1997).
- [33] T. Pandiyan, S. Bernès and C. Durán de Bazúa, *Polyhedron* **16**, 2819 (1997).
- [34] Y. Nakao, C. Mori, W. Mori, T. Sakurai, K. Matsumoto and H. Kimoto, *Chem. Lett.* 641 (1996).
- [35] D. Volkmer, B. Hommerich, K. Griesar, W. Haase and B. Krebs, *Inorg. Chem.* **35**, 3792 (1996).
- [36] A.P.B. Lever, *Studies in Physical and Theoretical Chemistry* (Elsevier Science, New York, 1984), Vol. 33, p. 507.
- [37] B.N. Figgis and M.A. Hitchman, *Ligand Field Theory and its Applications* (Wiley-VCH, New York, 2000).
- [38] H.P. Berends and D.W. Stephan, *Inorg. Chim. Acta* **93**, 173 (1984).
- [39] T. Pandiyan, S. Bernès and C. Durán de Bazúa, *Acta Crystallogr.* **C53**, 1607 (1997).